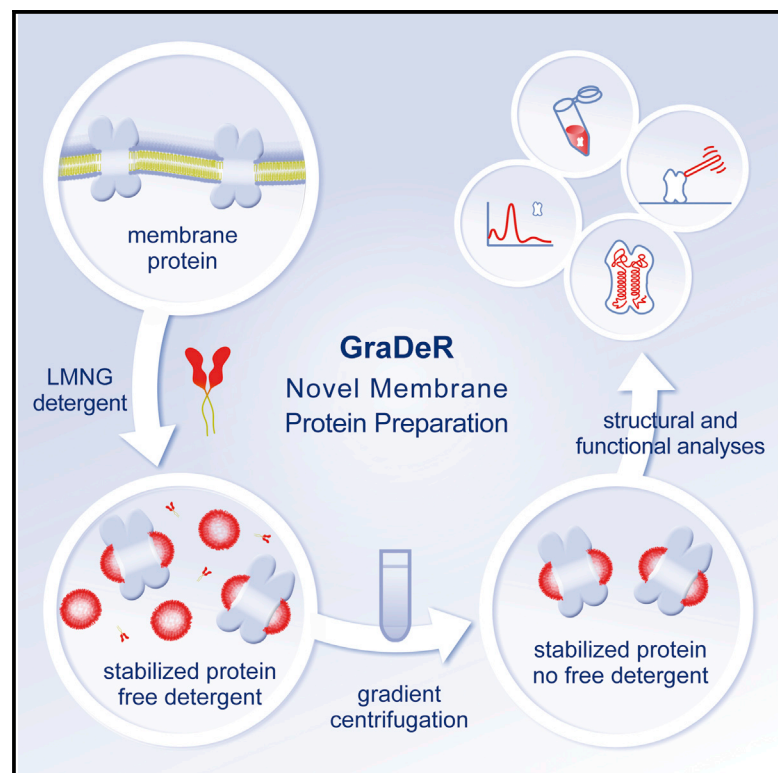# GraDeR: Membrane Protein Complex Preparation for Single-Particle Cryo-EM

Graphical Abstract

Authors

Florian Hauer, Christoph Gerle, Niels Fischer, ..., Ken Yokoyama, Yoshinori Fujiyoshi, Holger Stark

Correspondence

hstark1@gwdg.de (H.S.),
gerle.christoph@gmail.com (C.G.)

In Brief

While single-particle cryo-EM has emerged as a powerful technique for structure determination of membrane proteins, cryo-EM sample preparation remains the major bottleneck. Hauer et al. describe a novel, widely applicable approach that significantly improves sample quality of membrane proteins for structural analysis by cryo-EM.

Highlights

- GraDeR protocol mildly removes free detergent from membrane protein complexes

- GraDeR facilitates cryo-EM analysis of membrane protein complexes

- GraDeR improves stability of fragile multisubunit membrane complexes

- Structural evidence for Boyer's binding change mechanism in intact F-ATP synthase

CrossMark

CellPress

GraDeR: Membrane Protein Complex Preparation for Single-Particle Cryo-EM

Florian Hauer,[1,7] Christoph Gerle,[2,3,7,*] Niels Fischer,[1,7] Atsunori Oshima,[4] Kyoko Shinzawa-Itoh,[2] Satoru Shimada,[2] Ken Yokoyama,[5] Yoshinori Fujiyoshi,[4] and Holger Stark[1,6,*]

[1]3D Electron Cryomicroscopy Group, Max Planck Institute for Biophysical Chemistry, Am Fassberg 11, 37077 Göttingen, Germany
[2]Department of Life Science, Picobiology Institute, Graduate School of Life Science, University of Hyogo, 3-2-1 Kouto, Kamigori, Ako, Hyogo 678-1297, Japan
[3]Japan Science and Technology Agency (JST), Core Research for Evolutional Science and Technology (CREST), Kawaguchi 332-0012, Japan
[4]Cellular and Structural Physiology Institute, Nagoya University, Chikusa-ku, Nagoya 464-8601, Japan
[5]Department of Molecular Biosciences, Kyoto Sangyo University, Kamigamo Motoyama, Kita-ku, Kyoto 603-8555, Japan
[6]Department of 3D Electron Cryomicroscopy, Institute of Microbiology and Genetics, Georg-August Universität, 37077 Göttingen, Germany
[7]Co-first author
*Correspondence: hstark1@gwdg.de (H.S.), gerle.christoph@gmail.com (C.G.)
http://dx.doi.org/10.1016/j.str.2015.06.029

SUMMARY

We developed a method, named GraDeR, which substantially improves the preparation of membrane protein complexes for structure determination by single-particle cryo-electron microscopy (cryo-EM). In GraDeR, glycerol gradient centrifugation is used for the mild removal of free detergent monomers and micelles from lauryl maltose-neopentyl glycol detergent stabilized membrane complexes, resulting in monodisperse and stable complexes to which standard processes for water-soluble complexes can be applied. We demonstrate the applicability of the method on three different membrane complexes, including the mammalian F_oF_1 ATP synthase. For this highly dynamic and fragile rotary motor, we show that GraDeR allows visualizing the asymmetry of the F_1 domain, which matches the ground state structure of the isolated domain. Therefore, the present cryo-EM structure of F_oF_1 ATP synthase provides direct structural evidence for Boyer's binding change mechanism in the context of the intact enzyme.

INTRODUCTION

Integral membrane proteins (IMPs) constitute ~30% of the proteome (Wallin and Heijne, 1998) and represent the majority of pharmaceutical targets (Overington et al., 2006). Despite their biological and medical relevance, our understanding of the structure and function of IMPs lags far behind that of water-soluble protein complexes. Cryo-electron microscopy (cryo-EM) has become a powerful tool to determine the structure of macromolecular complexes (Bai et al., 2015) and has recently successfully been applied to obtain subnanometer resolution structures of IMPs, with sizes from several hundred kilodaltons (Liao et al., 2013; Kim et al., 2015; Meyerson et al., 2014; Paulsen et al., 2015) up to the megadalton range (Vinothkumar et al., 2014; Allegretti et al., 2015; Efremov et al., 2014; Yan

et al., 2014; Zalk et al., 2015). However, cryo-preparation of membrane protein complexes remains tedious and represents the major bottleneck for 3D structure determination by cryo-EM (Rubinstein, 2007; Schmidt-Krey and Rubinstein, 2011; Liao et al., 2014).

The major challenge for cryo-EM and most other experimental methods in probing the structure and function of IMPs is the need to extract the IMPs from their native cellular environment (the membrane) and to obtain water-soluble, monodisperse, and stable protein complexes. For the removal of IMPs from the membrane by amphiphilic detergents, the detergent has to be used at a concentration above its critical micellar concentration (CMC), resulting in three challenges: (1) free detergent can result in lower image contrast by cryo-EM, and detergent micelles can be mistaken for protein particles in electron micrographs (Rubinstein, 2007) (Figures S1A and S1B); (2) high concentrations of free detergent monomers complicate the controlled formation of thin ice required for cryo-EM grid preparation (Schmidt-Krey and Rubinstein, 2011); and (3) detergent binding to the IMP lipophilic surface in the protein-detergent complex (Popot, 2010) affects image processing (Baker et al., 2012). Alternative approaches avoid these problems by using amphiphilic polymers (Tribet et al., 1996), amphipols, protein caged lipid bilayers, nanodiscs (Nath et al., 2007), or engineered β-sheet peptides (Tao et al., 2013). Notably, the first atomic resolution model of an IMP by single-particle cryo-EM was obtained from protein stabilized by amphipol in the absence of detergent (Cao et al., 2013). However, whereas all the aforementioned approaches were successfully applied to some IMPs, none of them is universally applicable and each one may require extensive optimization. Here, we present the gradient-based detergent removal (GraDeR) approach as a broadly applicable technique to prepare IMPs for cryo-EM studies.

RESULTS AND DISCUSSION

GraDeR: Gradient-Based Detergent Removal
GraDeR enables the gentle removal of free detergent micelles and detergent monomers from IMPs stabilized with lauryl

Table 1. Procedures to Remove Free LMNG and Associated Issues

Procedure to Remove Free LMNG[a]	Issues
Dialysis	lengthy
BioBeads	incomplete removal
Size-exclusion chromatography (long, HPLC)	damage of fragile IMPs by (1) loss of lipids and/or (2) loss of IMP bound LMNG through resin absorbance
Size-exclusion chromatography (short, gravimetric, or spin)	co-migration of LMNG micelles
Precipitation (by e.g. PEG6000)	co-precipitation of LMNG micelles
Sedimentation	potential co-sedimentation of LMNG micelles and loss of monodispersity (see precipitation)
Cyclodextrin complexation	difficult calibration (Signorell et al., 2007)
Density gradient centrifugation (GraDeR)	none

HPLC, high-performance liquid chromatography.

[a]Manifold methods can be used to separate free LMNG from LMNG-stabilized IMPs. However, especially for fragile IMPs, alternative methods to density gradient centrifugation exhibited specific issues, mainly originating from the very slow kinetics of free monomer to free micelle exchange, which impeded their use for single-particle cryo-EM.

maltose-neopentyl glycol (LMNG or MNG-3), a member of a new maltose-neopentyl glycol class of amphiphiles (Chae et al., 2010). Absence of free detergent micelles usually leads to the rapid desorption of detergent from the protein-detergent complex, resulting in rapid aggregation of IMPs (Rasmussen et al., 2011). However, LMNG exhibits an extremely slow off-rate, four orders of magnitude lower than that of commonly used dodecyl maltoside (DDM) (Chung et al., 2012). The high stability of LMNG detergent micelles (Figure S1A) precludes detergent removal by conventional methods such as dialysis or BioBeads adsorption, and the extremely low CMC of LMNG renders simple dilution unfeasible. Furthermore, chromatography-based separation methods for buffer exchange frequently destabilize membrane protein complexes of higher organisms by removing native, structurally bound lipids. Table 1 summarizes the different approaches for removal of free detergent tested by us and the observed issues that preclude their use, in particular for fragile multidomain membrane complexes. We demonstrate, however, that free detergent micelles and detergent monomers can be efficiently and mildly removed by glycerol gradient centrifugation by applying an additional gradient of LMNG that is inverse to the glycerol gradient (Figure 1). To investigate its general applicability, we tested GraDeR on three functionally and structurally divergent IMPs from evolutionarily distant organisms. In all three cases, GraDeR efficiently removed free LMNG micelles and monomers from the IMP-LMNG preparation, resulting in monodisperse and stable IMP preparations with surface tension similar to that of detergent-free solutions (Figure S2). Importantly, GraDeR highly improved the behavior of the IMPs in cryo-EM preparation and imaging.

Cryo-EM Preparation of Bacterial V-ATPase by GraDeR

As a first test case, we investigated the V-ATPase from the thermophilic eubacteria *Thermus thermophilus*. *T. thermophilus* V-ATPase is an energy-converting rotary nanomotor (Toei et al., 2007) and was the first membrane protein to be characterized by single-particle cryo-EM at a resolution sufficient to resolve α helices (Lau and Rubinstein, 2012). When V-ATPase was solubilized in DDM, the success rate in preparation of cryo-EM grids was very low. Despite using a direct electron detector for image acquisition, an estimated 95% of all cryo-EM grids were not suitable for further cryo-EM analysis (Figure 2A, left) and a grid that was recorded on a conventional CCD camera showed the best contrast for particles (Figure S1C). In contrast, using the GraDeR protocol, thin ice with a favorable distribution of monodisperse V-ATPases exhibiting enhanced contrast was readily formed, resulting in a substantially larger fraction of grids suitable for cryo-EM analysis (>20%) (Figure 2A, right). Furthermore, instead of the heterogeneous background typically observed in vitreous ice of cryo-EM preparations containing detergent micelles (Lu et al., 2014) (Figure 2A, left; Figure S1C), the ice appeared more homogeneous (Figure 2A, right). Thus, new-generation direct electron detectors, which generally allow obtaining images at high signal-to-noise ratio, do not allow the limitations set by the quality of the cryo-preparation to be overcome. Furthermore, when we compared class averages of the best DDM dataset and a typical GraDeR dataset, the relative number of class averages suitable for further image processing was significantly higher in the GraDeR dataset (Figure 2B). Interestingly, the GraDeR dataset also had a much lower number of class averages of broken V-ATPase, indicating that LMNG, even in the absence of free detergent micelles, is more apt to stabilize the fragile IMP than is DDM.

GraDeR Preparation of Nematode Innexin-6

Secondly, we successfully applied GraDeR to Innexin-6 from the nematode *Caenorhabditis elegans*. Innexin-6 is a member of the gap junctions, which are important components of cell-to-cell communication in multicellular organisms (Oshima, 2014). In micrographs of negatively stained Innexin-6 hemi-channels solubilized in LMNG, the LMNG detergent micelles appear as protein-like globular densities (Figure 2C, top), similar to the ones observed in protein free buffer including LMNG (Figure S1A). Innexin-6 hemi-channels prepared by GraDeR were stable and monodisperse, and the background was completely free of detergent micelles (Figure 2C, bottom), demonstrating the suitability of GraDeR also for an IMP from a multicellular organism with a natural environment at ambient temperature.

3D Cryo-EM Analysis of Mammalian F_oF_1 ATP Synthase Using GraDeR

A very recent cryo-EM study of the extraordinary stable and large ($\sim$1.6 MDa) *Polytomella* F_oF_1 ATP synthase dimer revealed the unusual and functionally important horizontal α-helical architecture of its stator a-subunit (Allegretti et al., 2015). This study demonstrates the power of cryo-EM to analyze the structure of intact F_oF_1 ATP synthases, which have resisted structural investigation by crystallographic means for decades. Therefore, we also tested GraDeR on the substantially smaller and very fragile $\sim$600-kDa mammalian F_oF_1 ATP synthase from *Bos taurus*.
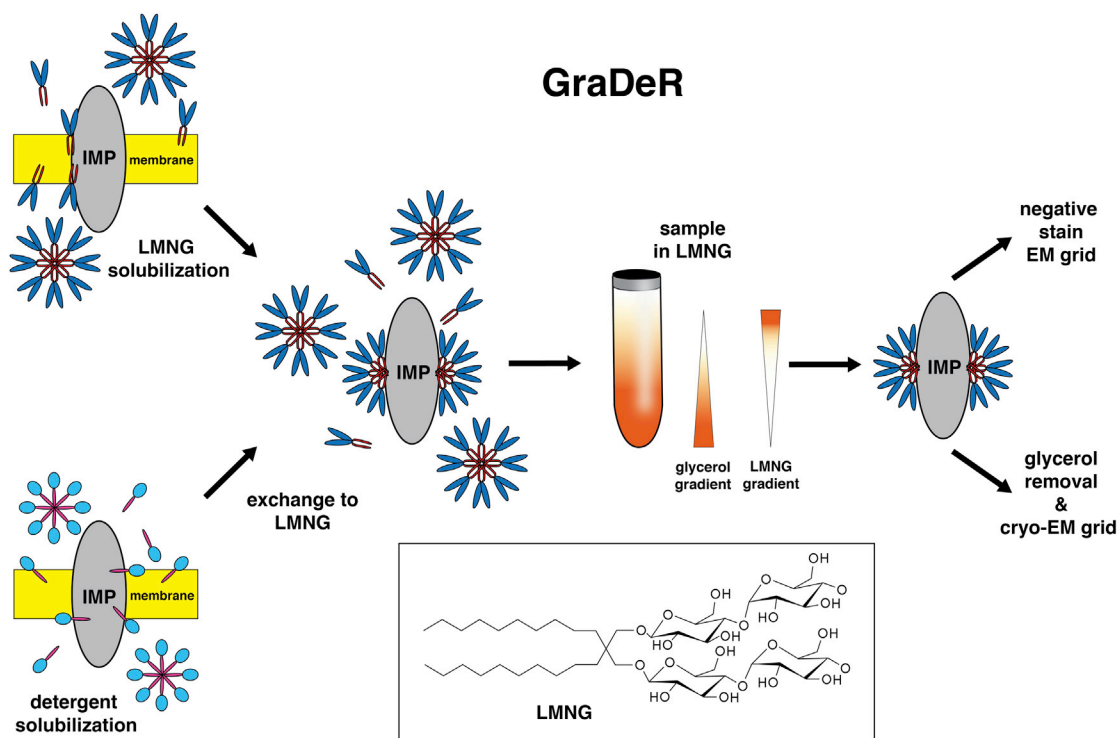
GraDeR

Figure 1. GraDeR Workflow

IMPs are solubilized in lauryl maltose-neopentyl glycol (LMNG) either by direct extraction or after exchange from another detergent. Free LMNG detergent micelles and monomers are removed by gradient centrifugation. LMNG-stabilized IMP in the absence of free detergent micelles and monomers can be used for single-particle cryo-EM. Inset: Chemical structure of LMNG, which is basically that of two fused dodecyl-maltoside molecules. The combination of a lipid-like hydrophobic tail and a hydrophilic headgroup big enough to prevent the formation of bilayers, together with a central, stiff quaternary carbon bond, convey LMNG with remarkable chemical properties (Chae et al., 2010).

This highly dynamic rotary nanomachine is central to ATP formation in the mammalian cell, comprising 17 different subunits, some of which are easily lost during purification and sample preparation (Runswick et al., 2013). GraDeR-prepared F_oF_1 ATP synthase remained monodisperse and stable for more than 2 days at 4°C. In contrast to the V-ATPase from a thermophile bacterium and the nematode Innexin-6 gap junction channels, however, mammalian F_oF_1 ATP synthase was sensitive to the blotting process during cryo-grid preparation (Figure 3A), likely due to shear stress caused by fast blotting with cellulose. Therefore, we used nitrocellulose for blotting, which absorbs water about ten times slower than the cellulose filter papers conventionally used for blotting. In contrast to cellulose blotting, nitrocellulose blotting resulted in cryo-EM grids with intact complexes (Figure 3B). The use of nitrocellulose may be generally beneficial for cryo-grid preparation of fragile IMPs and other weakly associated macromolecular complexes.

To establish whether the observed improvements in cryo-EM preparation by GraDeR directly correlate with improved 3D cryo-EM maps, we performed 3D cryo-EM analysis of the bovine F_oF_1 ATP synthase. Recent cryo-EM preparations of bovine F_oF_1 ATP synthase have used DDM as detergent, resulting in the currently best-resolved cryo-EM map of bovine F_oF_1 ATP synthase at 18 Å resolution (Baker et al., 2012). Using GraDeR, we were able to obtain a well-defined 3D cryo-EM map of bovine F_oF_1 ATP synthase at 11 Å resolution (Figures 3C–3E; Figure S3;

Supplemental Experimental Procedures). The present map allowed reliable docking of subcomplex crystal structures. The asymmetry in the C-terminal domain of the catalytic $(\alpha\beta)_3$ hexamer generally fits the ground state structure of the isolated F_1 domain (Abrahams et al., 1994), enabling us to confidently assign the catalytic $\alpha\beta$ pairs E, TP, and DP (Figures 3D and 3E). As a consequence, the present 3D reconstruction gives direct structural evidence of Boyer's binding change mechanism in the context of the intact F_oF_1 ATP synthase. Boyer's binding change mechanism of rotary catalysis requires that during its reaction cycle the catalytic subunits of the ATP synthase are in different conformational states at any given time (Boyer, 1997). However, our structure also shows rearrangements of the central stalk's globular domain and the α_E and the β_{DP} subunit in comparison with the crystal structure. In particular, the foot of the central stalk is rotated counter-clockwise by about 30°. This rotational flexibility supports the notion of the globular domain of the central stalk acting as a pliable element in elastic power transmission between the F_o and F_1 rotary stepping motor (Sielaff et al., 2008). Furthermore, α_E and β_{DP} shift away from the central γ subunit and interact with the peripheral stalk, which is not present in the F_1 crystal structure. Recently a contact between peripheral stalk and the lower domain of α_E was also observed for the membrane-embedded bovine holoenzyme (Jiko et al., 2015). In line with the results of a crosslinking study on the bacterial F_oF_1 holoenzyme in synthesis mode (Masaike et al., 2006), this
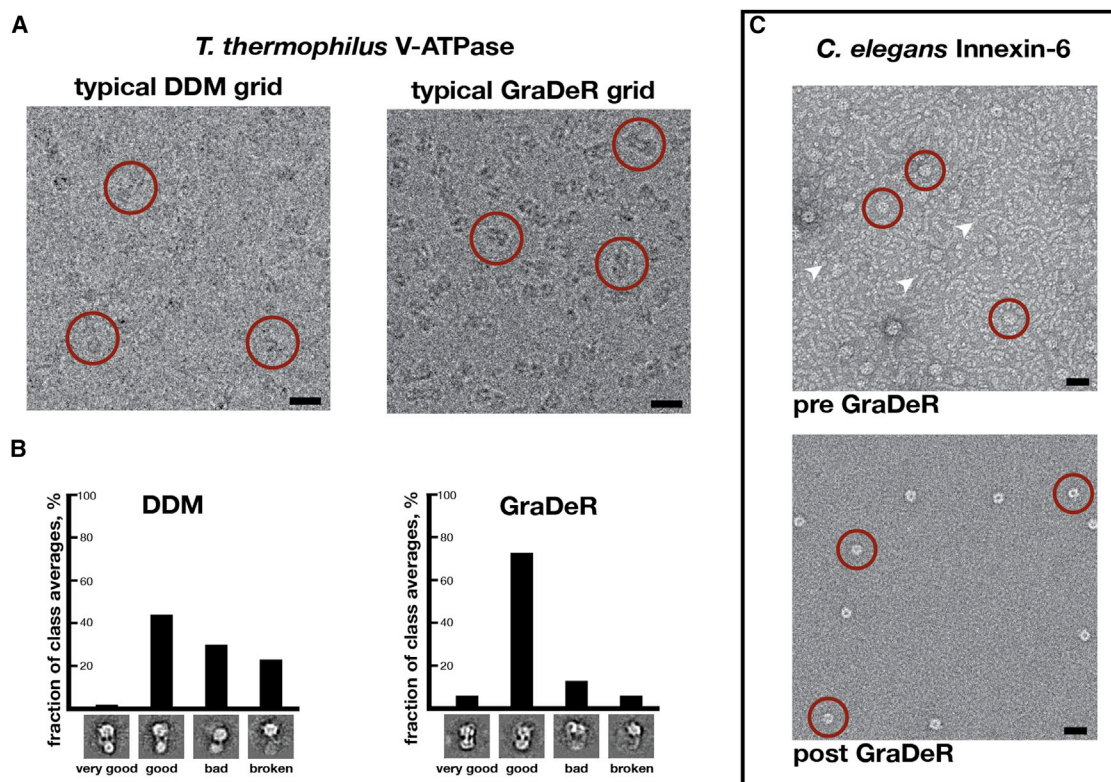
Figure 2. Impact of GraDeR on Different Membrane Protein Complexes

(A) Cryo-EM images of *T. thermophilus* V-ATPase without and with GraDeR treatment, both obtained using a direct electron detector. The majority of standard cryo-EM grids of DDM-solubilized complexes were not suitable for data acquisition and processing (>95%) (left), whereas a large portion (>20%) of GraDeR-prepared cryo-EM grids exhibited good particle contrast (right). Fractions (in percent) were estimated based on analysis of ≥60 (DDM) and ≥20 (GraDeR) grids. Exemplary V-ATPase complexes are circled in red. Scale bars, 20 nm.

(B) Distribution of class average qualities for the best cryo-EM dataset of DDM-solubilized V-ATPase (left) versus a typical V-ATPase cryo-EM dataset obtained by GraDeR treatment (right). For the dataset of DDM-solubilized V-ATPase, 1,500 class averages were calculated from 49,000 images; for the dataset derived from GraDeR treatment, 1,400 class averages were calculated from a total of 46,000 images.

(C) Negative stain images of *C. elegans* Innexin-6 hemi-channels before (top) and after GraDeR treatment (bottom). Note the absence of LMNG micelles after GraDeR treatment (bottom). Exemplary hemi-channels are circled in red, exemplary LMNG micelles are indicated by white arrowheads. Scale bars, 20 nm.

rearrangement of α_E and β_{DP} increases the distance between the C-terminal domains of the β subunits in the TP and DP sites, implying that mitochondrial F_oF_1 ATP synthase in mammals might be structurally biased toward ATP synthesis.

Conclusions

In summary, the present results demonstrate the ability of GraDeR to produce stable, monodisperse IMPs in the absence of free detergent, and its usefulness in the preparation of grids for structural analysis by single-particle cryo-EM. Successful application of GraDeR to IMPs from divergent sources shows its broad applicability. GraDeR increases the success rate of obtaining viable cryo-preparations for single-particle EM and allows the application of well-established procedures for water-soluble protein complexes to IMPs. In addition, procedural similarity to GraFix (Kastner et al., 2008) makes it possible to combine GraDeR and GraFix in one experimental step by simply including a chemical fixation reagent of choice during gradient centrifugation (Figure S4). Combining GraDeR with GraFix allows even more stabilization of highly fragile multidomain membrane complexes, further enhancing the versatility of our approach.

We expect GraDeR to significantly boost the applicability of cryo-EM for the structural analysis of fragile and dynamic membrane protein complexes. The general capability of GraDeR to remove micelles and free detergent, while keeping IMPs stable and monodisperse, should also facilitate analysis by other structural and biochemical methods such as mass spectrometry, X-ray crystallography, and single-molecule techniques.

EXPERIMENTAL PROCEDURES

Membrane Protein Preparation

Although direct solubilization by LMNG is feasible for some IMPs, e.g. the TRPA1 channel (Paulsen et al., 2015) or gastric H^+,K^+-ATPase (K. Abe, personal communication), in this study all three membrane complexes employed were first solubilized by another detergent, which was then exchanged for LMNG during the final purification step as described below. In all cases shown, the slow kinetics of LMNG made it necessary to conduct the exchange slowly. LMNG stock solutions (10%) were prepared by gently mixing LMNG with MilliQ water at 50°C for 12 hr.

T. thermophilus V-ATPase was isolated from *T. thermophilus* membranes as previously described (Gerle et al., 2006) with the following modifications. After solubilization of membranes with Triton X-100, followed by purification using Ni-nitrilotriacetic acid (NTA) affinity chromatography, the V-ATPase solution
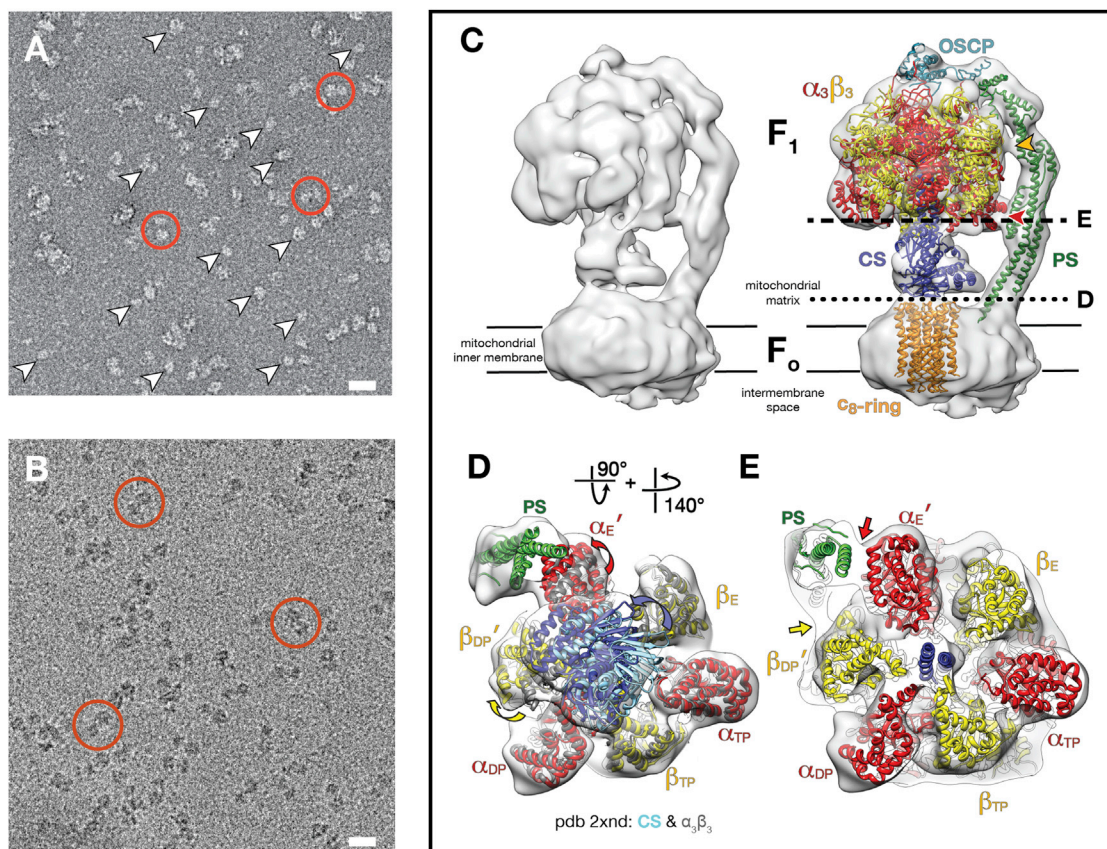
Figure 3. Cryo-EM Reconstruction of Mammalian F$_o$F$_1$ ATP Synthase

(A) Negatively stained bovine F$_o$F$_1$ ATP synthase after cryo-grid blotting using conventional cellulose blotting paper. Some intact complexes are circled in red. White arrowheads indicate debris from broken F$_o$F$_1$ complexes. Scale bars, 20 nm.

(B) Typical cryo-EM grid of GraDeR-prepared bovine F$_o$F$_1$ ATP synthase using nitrocellulose for slow blotting of excess buffer before plunge-freezing. All bovine F$_o$F$_1$ ATP synthase complexes in the image appear to be intact. Exemplary complexes are encircled in red. Scale bar, 20 nm.

(C) Cryo-EM 3D reconstruction of bovine F$_o$F$_1$ ATP synthase without (left) and with fitted subcomplex X-ray crystal structures (PDB: 2XND, 2CLY, and 2WSS). A yellow and a red arrowhead indicate a contact of β$_{DP}$ and α$_E$, respectively, with the peripheral stalk (PS). A dotted line indicates the cross section shown in (D) and a dashed line the cross section in (E).

(D) Rearrangements of the catalytic hexamer and central stalk in intact F$_o$F$_1$ ATP synthase (view from the membrane side). Colored arrows indicate the re-arrangements of α$_E$ (yellow), β$_{DP}$ (red), and the central stalk (blue) in comparison with the crystal structure of the subcomplex (PDB: 2XND) comprising the catalytic hexamer (dark gray), central stalk (sky blue), and c$_8$-ring (not shown).

(E) Interactions between the catalytic hexamer and the peripheral stalk (PS) (view from the membrane side). α$_E$ and β$_{DP}$ interact with the peripheral stalk (colored arrows) increasing the distance between β$_{DP}$′ and β$_{TP}$ in comparison with the subcomplex (PDB: 2XND).

was applied to a 6-ml Resource Q (Amersham) anion exchange column. Detergent exchange to LMNG was performed on the column by washing with a double gradient from 0.05% to 0% Triton X-100 and 0%–0.05% LMNG for 100 min at a flow rate of 0.5 ml/min and subsequent NaCl gradient elution by an LMNG (0.05%)-containing buffer (20 mM Tris-HCl [pH 8.0], 0.1 mM EDTA, 0–500 mM NaCl, 0.05% LMNG).

C. elegans Innexin-6 gap junction channels were expressed and purified from Sf9 cells as previously described (Oshima et al., 2013) with the following modifications. Cell membranes were solubilized with 2% DDM and purified by Ni-NTA affinity chromatography with buffers for wash and elution including 0.1% digitonin. Digitonin was exchanged to LMNG by performing gel filtration on a Superose 6 column using a running buffer containing 0.02% LMNG (10 mM Tris-HCl [pH 7.5], 150 mM NaCl, 0.02% LMNG).

Bovine F$_o$F$_1$ ATP synthase was purified as reported (Maeda et al., 2013) with the following modifications. After sucrose density gradient centrifugation and binding to a Poros 20-HQ anion exchange resin, exchange from decyl-malto-side to LMNG was achieved by washing with a double gradient from 0.2% to 0% decyl-maltoside and 0%–0.05% LMNG for 80 min at 1 ml/min and subse-

quent elution with a buffer containing 0.05% LMNG (40 mM HEPES-Na [pH 7.8], 0–240 mM KCl, 150 mM sucrose, 2 mM MgCl$_2$, 0.1 mM DTT, 0.1 mM EDTA, 0.05% LMNG).

All LMNG-stabilized IMP solutions were dispensed into small aliquots of less than 500 μl, flash-frozen in liquid nitrogen, and stored at −80°C until further use.

Density Gradient Centrifugation

Density gradients were prepared such that the protein complexes migrate two-thirds down the tube, reaching a final detergent concentration below the CMC. We typically adjust the detergent gradient at three times the CMC (0.003% LMNG) at the top of the gradient to 0% at the bottom of the tube. The linear detergent gradient serves the purpose of stabilizing protein-bound micelles during long centrifugation runs (>12 hr). The GraDeR protocol has been tested at 4°C. At higher temperatures, we expect a higher off-rate of LMNG from the protein-detergent complex below CMC.

Gradients were prepared following standard procedures (Kastner et al., 2008). In brief, filtered buffer solutions containing crowding agents (we

routinely use glycerol or sucrose) at high and low concentrations were prepared in plastic tubes. 0.003% LMNG (Anatrace) was added to the low-density solution, and gradients were prepared using a gradient former (Gradient Master 107, BioComp Instruments) following standard procedures. We routinely run 4-ml gradients in TH-660 (Kendro Laboratory Products) swing-out rotors (equivalent to Beckman SW60 rotors). Centrifugation times from 3 to 18 hr and speeds of 20,000 to 60,000 rpm have been used depending on the size of the complex. In particular, V-ATPase was run in a gradient containing 50 mM HEPES (pH 8.0) and 150 mM NaCl, with a density/LMNG gradient ranging from 10% glycerol and 0.003% LMNG at the top to 40% glycerol at the bottom. The gradient was run in an SW60 rotor at 38,000 rpm (194,559 × g) for 18 hr. F_oF_1 ATP synthase was run in a gradient containing 50 mM HEPES (pH 8.0), 100 mM NaCl, 0.1% azide, 0.5 mM ADP, and 5 mM $MgCl_2$, with a density/LMNG gradient ranging from 10% glycerol and 0.003% LMNG at the top to 30% glycerol at the bottom. The gradient was run in an SW60 rotor at 38,000 rpm (194,559 × g) for 12 hr. Innexin-6 was run in a gradient containing 10 mM Tris-HCl (pH 7.5) and 150 mM NaCl, with a density/LMNG gradient ranging from 10% glycerol and 0.003% LMNG at the top to 30% glycerol at the bottom. The gradient was run in an SW60 rotor at 33,000 rpm (146,728 × g) for 18 hr. All gradients were run at 4°C.

After gradient centrifugation, the gradient was fractionated from the bottom to the top, as residual detergent micelles at the top of the gradient might contaminate the preparation.

Buffer Exchange

After gradient fractionation, it is necessary to remove the crowding agent (i.e. glycerol or sucrose) prior to preparation of cryo-EM grids. To successfully remove residual LMNG from the buffer solution, LMNG needs to be below the CMC, otherwise the highly stable micelles will carry over during buffer exchange. We have successfully used buffer exchange protocols using spin columns (Pierce), gravity columns (GE Healthcare), and dialysis to remove glycerol. The choice of buffer exchange method, however, should be made with regard to the stability of the complex, with dialysis being the gentlest method. IMPs whose stability depends on the presence of lipids tend to be sensitive to contact with resin material, so dialysis should be the preferred method of buffer exchange. Specifically, we used Zeba Spin Desalting Columns, 40K MWCO (Thermo Fisher) following the supplier's protocol for V-type ATPase and Innexin. For the V-type ATPase, PD Mini-Trap G-25 desalting columns (GE Healthcare) following the gravity protocol provided by the supplier have been used successfully as well. Buffer exchange in F_oF_1 ATP synthase has been done by dialysis using a SpectraPor No. 7 (MWCO 50,000) membrane following standard procedures.

3D Cryo-EM Analysis of Mammalian F_1F_o-ATP Synthase

After removal of excess LMNG by the GraDeR protocol, cryo-EM grids of bovine F_oF_1 ATP synthase were prepared as described by Kastner et al. (2008) with modifications. Importantly, nitrocellulose paper was used instead of standard filter paper for manual blotting of excess solution directly prior to plunge-freezing to prevent the known disintegration of the fragile mammalian F_oF_1 ATP synthase by fast blotting of excess liquid. Particles were then imaged under liquid nitrogen conditions on a 4k × 4k Falcon II direct electron detector in a Titan Krios electron microscope (both FEI Company) at 300 kV acceleration voltage, an exposure of about 45 electrons/$Å^2$, 2.5–5 μm defocus, and 94,000-fold nominal magnification, corresponding to a final pixel size of 1.6 Å. Individual particle images were selected semi-automatically and corrected locally for the contrast transfer function (Sander et al., 2003), resulting in ~50,000 particle images. Subsequent 3D classification yielded a homogeneous group of 13,000 good-quality F_oF_1 ATP synthase particles from which a 3D reconstruction was computed at 11 Å resolution. The resolution was determined using independently refined half datasets according to the original definition of the Fourier-shell correlation (FSC) procedure (Harauz and van Heel, 1986), also termed gold-standard FSC (Scheres, 2012), using a soft shaped mask (Figure S3A). For interpretation, the final cryo-EM map was amplitude sharpened and low-pass filtered at 11 Å. Image processing was performed using Imagic-5 (van Heel et al., 1996), custom-made software (B.B., M.L., and H.S., unpublished data), and Relion 1.3 (Scheres, 2012).

REFERENCES

Abrahams, J.P., Leslie, A.G., Lutter, R., and Walker, J.E. (1994). Structure at 2.8 Å resolution of F1-ATPase from bovine heart mitochondria. Nature *370*, 621–628.

Allegretti, M., Klusch, N., Mills, D.J., Vonck, J., Kühlbrandt, W., and Davies, K.M. (2015). Horizontal membrane-intrinsic α-helices in the stator a-subunit of an F-type ATP synthase. Nature *521*, 237–240.

Bai, X.-C., McMullan, G., and Scheres, S.H.W. (2015). How cryo-EM is revolutionizing structural biology. Trends Biochem. Sci. *40*, 49–57.

Baker, L.A., Watt, I.N., Runswick, M.J., Walker, J.E., and Rubinstein, J.L. (2012). Arrangement of subunits in intact mammalian mitochondrial ATP synthase determined by cryo-EM. Proc. Natl. Acad. Sci. USA *109*, 11675–11680.

Boyer, P.D. (1997). The ATP synthase—a splendid molecular machine. Annu. Rev. Biochem. *66*, 717–749.

Cao, E., Liao, M., Cheng, Y., and Julius, D. (2013). TRPV1 structures in distinct conformations reveal activation mechanisms. Nature *504*, 113–118.

Chae, P.S., Rasmussen, S.G.F., Rana, R.R., Gotfryd, K., Chandra, R., Goren, M.A., Kruse, A.C., Nurva, S., Loland, C.J., Pierre, Y., et al. (2010). Maltose-neopentyl glycol (MNG) amphiphiles for solubilization, stabilization and crystallization of membrane proteins. Nat. Methods *7*, 1003–1008.

Chung, K.Y., Kim, T.H., Manglik, A., Alvares, R., Kobilka, B.K., and Prosser, R.S. (2012). Role of detergents in conformational exchange of a G protein-coupled receptor. J. Biol. Chem. *287*, 36305–36311.

Efremov, R.G., Leitner, A., Aebersold, R., and Raunser, S. (2014). Architecture and conformational switch mechanism of the ryanodine receptor. Nature *517*, 39–43.

Gerle, C., Tani, K., Yokoyama, K., Tamakoshi, M., Yoshida, M., Fujiyoshi, Y., and Mitsuoka, K. (2006). Two-dimensional crystallization and analysis of projection images of intact *Thermus thermophilus* V-ATPase. J. Struct. Biol. *153*, 200–206.

Harauz, G., and van Heel, M. (1986). Exact filters for general geometry three dimensional reconstruction. Optik *73*, 146–156.

Jiko, C., Davies, K.M., Shinzawa-Itoh, K., Tani, K., Maeda, S., Mills, D.J., Tsukihara, T., Fujiyoshi, Y., Kühlbrandt, W., and Gerle, C. (2015). Bovine F1Fo ATP synthase monomers bend the lipid bilayer in 2D membrane crystals. Elife *4*, e06119.

Kastner, B., Fischer, N., Golas, M.M., Sander, B., Dube, P., Boehringer, D., Hartmuth, K., Deckert, J., Hauer, F., Wolf, E., et al. (2008). GraFix: sample preparation for single-particle electron cryomicroscopy. Nat. Methods *5*, 53–55.

Kim, J., Wu, S., Tomasiak, T.M., Mergel, C., Winter, M.B., Stiller, S.B., Robles-Colmanares, Y., Stroud, R.M., Tampé, R., Craik, C.S., et al. (2015). Subnanometre-resolution electron cryomicroscopy structure of a heterodimeric ABC exporter. Nature *517*, 396–400.

Lau, W., and Rubinstein, J. (2012). Subnanometre-resolution structure of the intact *Thermus thermophilus* H$^+$-driven ATP synthase. Nature *481*, 214–218.

Liao, M., Cao, E., Julius, D., and Cheng, Y. (2013). Structure of the TRPV1 ion channel determined by electron cryo-microscopy. Nature *504*, 107–112.

Liao, M., Cao, E., Julius, D., and Cheng, Y. (2014). Single particle electron cryo-microscopy of a mammalian ion channel. Curr. Opin. Struct. Biol. *27*, 1–7.

Lu, P., Bai, X.-C., Ma, D., Xie, T., Yan, C., Sun, L., Yang, G., Zhao, Y., Zhou, R., Scheres, S.H.W., et al. (2014). Three-dimensional structure of human γ-secretase. Nature *512*, 166–170.

Maeda, S., Shinzawa-Itoh, K., Mieda, K., Yamamoto, M., Nakashima, Y., Ogasawara, Y., Jiko, C., Tani, K., Miyazawa, A., Gerle, C., et al. (2013). Two-dimensional crystallization of intact F-ATP synthase isolated from bovine heart mitochondria. Acta Crystallogr. Sect. F Struct. Biol. Cryst. Commun. *69*, 1368–1370.

Masaike, T., Suzuki, T., Tsunoda, S.P., Konno, H., and Yoshida, M. (2006). Probing conformations of the β subunit of F0F1-ATP synthase in catalysis. Biochem. Biophys. Res. Commun. *342*, 800–807.

Meyerson, J.R., Kumar, J., Chittori, S., Rao, P., Pierson, J., Bartesaghi, A., Mayer, M.L., and Subramaniam, S. (2014). Structural mechanism of glutamate receptor activation and desensitization. Nature *514*, 328–334.

Nath, A., Atkins, W.M., and Sligar, S.G. (2007). Applications of phospholipid bilayer nanodiscs in the study of membranes and membrane proteins. Biochemistry *46*, 2059–2069.

Oshima, A. (2014). Structure and closure of connexin gap junction channels. FEBS Lett. *588*, 1230–1237.

Oshima, A., Matsuzawa, T., Nishikawa, K., and Fujiyoshi, Y. (2013). Oligomeric structure and functional characterization of *Caenorhabditis elegans* Innexin-6 gap junction protein. J. Biol. Chem. *288*, 10513–10521.

Overington, J.P., Al-Lazikani, B., and Hopkins, A.L. (2006). How many drug targets are there? Nat. Rev. Drug Discov. *5*, 993–996.

Paulsen, C.E., Armache, J.-P., Gao, Y., Cheng, Y., and Julius, D. (2015). Structure of the TRPA1 ion channel suggests regulatory mechanisms. Nature *520*, 511–517.

Popot, J.-L. (2010). Amphipols, nanodiscs, and fluorinated surfactants: three nonconventional approaches to studying membrane proteins in aqueous solutions. Annu. Rev. Biochem. *79*, 737–775.

Rasmussen, S.G.F., DeVree, B.T., Zou, Y., Kruse, A.C., Chung, K.Y., Kobilka, T.S., Thian, F.S., Chae, P.S., Pardon, E., Calinski, D., et al. (2011). Crystal structure of the β2 adrenergic receptor-Gs protein complex. Nature *477*, 549–555.

Rubinstein, J.L. (2007). Structural analysis of membrane protein complexes by single particle electron microscopy. Methods *41*, 409–416.

Runswick, M.J., Bason, J.V., Montgomery, M.G., Robinson, G.C., Fearnley, I.M., and Walker, J.E. (2013). The affinity purification and characterization of ATP synthase complexes from mitochondria. Open Biol. *3*, 120160.

Sander, B., Golas, M.M., and Stark, H. (2003). Automatic CTF correction for single particles based upon multivariate statistical analysis of individual power spectra. J. Struct. Biol. *142*, 392–401.

Scheres, S.H.W. (2012). RELION: implementation of a Bayesian approach to cryo-EM structure determination. J. Struct. Biol. *180*, 519–530.

Schmidt-Krey, I., and Rubinstein, J.L. (2011). Electron cryomicroscopy of membrane proteins: specimen preparation for two-dimensional crystals and single particles. Micron *42*, 107–116.

Sielaff, H., Rennekamp, H., Wächter, A., Xie, H., Hilbers, F., Feldbauer, K., Dunn, S.D., Engelbrecht, S., and Junge, W. (2008). Domain compliance and elastic power transmission in rotary F(O)F(1)-ATPase. Proc. Natl. Acad. Sci. USA *105*, 17760–17765.

Signorell, G.A., Kaufmann, T.C., Kukulski, W., Engel, A., and Rémigy, H.-W. (2007). Controlled 2D crystallization of membrane proteins using methyl-beta-cyclodextrin. J. Struct. Biol. *157*, 321–328.

Tao, H., Lee, S.C., Moeller, A., Roy, R.S., Siu, F.Y., Zimmermann, J., Stevens, R.C., Potter, C.S., Carragher, B., and Zhang, Q. (2013). Engineered nanostructured β-sheet peptides protect membrane proteins. Nat. Methods *10*, 759–761.

Toei, M., Gerle, C., Nakano, M., Tani, K., Gyobu, N., Tamakoshi, M., Sone, N., Yoshida, M., Fujiyoshi, Y., Mitsuoka, K., et al. (2007). Dodecamer rotor ring defines H$^+$/ATP ratio for ATP synthesis of prokaryotic V-ATPase from *Thermus thermophilus*. Proc. Natl. Acad. Sci. USA *104*, 20256–20261.

Tribet, C., Audebert, R., and Popot, J.-L. (1996). Amphipols: polymers that keep membrane proteins soluble in aqueous solutions. Proc. Natl. Acad. Sci. USA *93*, 15047–15050.

van Heel, M., Harauz, G., Orlova, E.V., Schmidt, R., and Schatz, M. (1996). A new generation of the IMAGIC image processing system. J. Struct. Biol. *116*, 17–24.

Vinothkumar, K.R., Zhu, J., and Hirst, J. (2014). Architecture of mammalian respiratory complex I. Nature *515*, 80–84.

Wallin, E., and Heijne, G.V. (1998). Genome-wide analysis of integral membrane proteins from eubacterial, archaean, and eukaryotic organisms. Protein Sci. *7*, 1029–1038.

Yan, Z., Bai, X.-C., Yan, C., Wu, J., Li, Z., Xie, T., Peng, W., Yin, C.-C., Li, X., Scheres, S.H.W., et al. (2014). Structure of the rabbit ryanodine receptor RyR1 at near-atomic resolution. Nature *517*, 50–55.

Zalk, R., Clarke, O.B., des Georges, A., Grassucci, R.A., Reiken, S., Mancia, F., Hendrickson, W.A., Frank, J., and Marks, A.R. (2015). Structure of a mammalian ryanodine receptor. Nature *517*, 44–49.

Supplemental Information

GraDeR: Membrane Protein Complex Preparation

for Single-Particle Cryo-EM

Florian Hauer, Christoph Gerle, Niels Fischer, Atsunori Oshima, Kyoko Shinzawa-Itoh, Satoru Shimada, Ken Yokoyama, Yoshinori Fujiyoshi, and Holger Stark
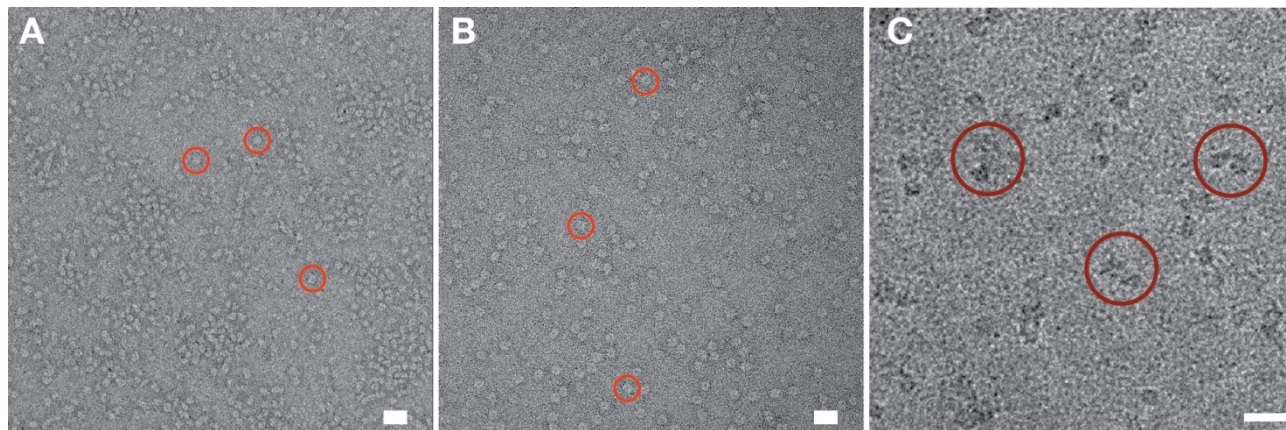
Supplemental Information

Supplemental Data

Figure S1, Related to Figure 1 and 2: Appearance of detergent micelles and small protein complexes in EM micrographs and best cryo-EM grid of DDM solubilized V-ATPase; scale bars 20 nm.

A) LMNG (0.02%) micelles in negative stain in the absence of protein. Red circles indicate individual LMNG micelles.

B) Protein complex heme-binding protein S (HbpS, 125 kDa) from *Streptomyces reticuli* in negative stain. Red circles denote exemplary HbpS complexes.

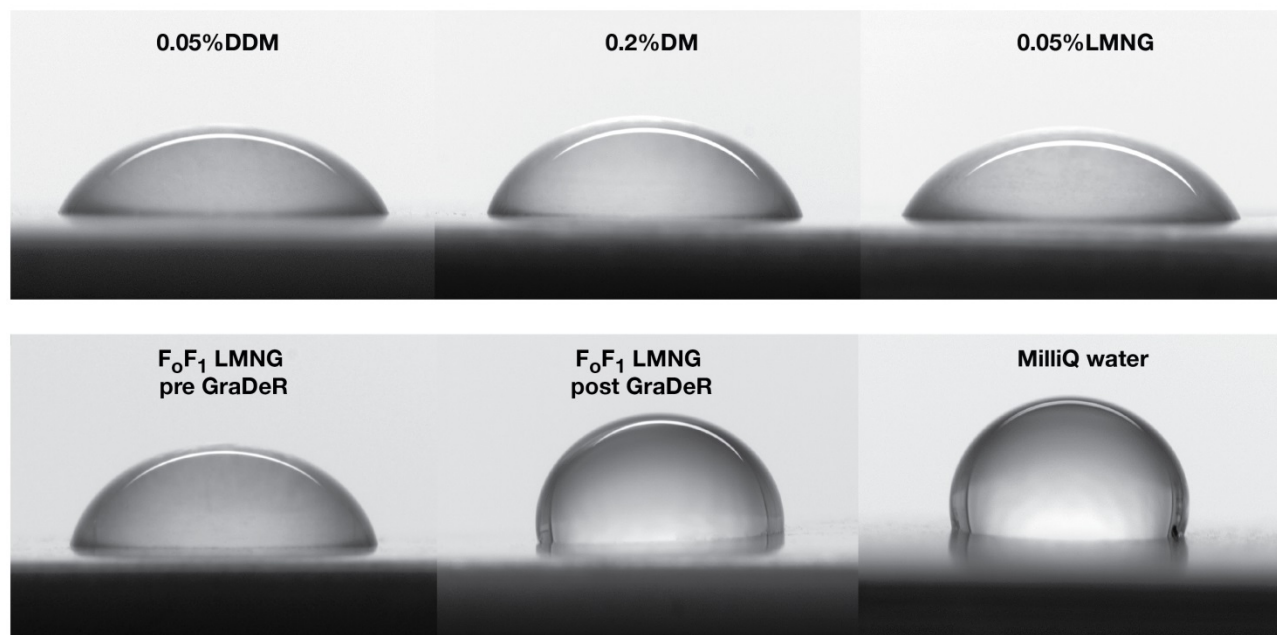C) Cryo-EM image of the best cryo-grid obtained for DDM-solubilized V-ATPase.

Figure S2, Related to Table 1: GraDeR and surface tension.

Drops of 20 µl buffer/water on freshly peeled Parafilm in the presence of detergent, F_oF_1-ATP synthase before GraDeR or after GraDeR and MilliQ water alone. Greater contact angle of the drop with the surface indicates stronger surface tension (Kaufmann et al., 2006), i.e. a lower concentration of surfactants at the air-water interface, which in turn corresponds to a lower surfactant monomer concentration in the bulk solution.
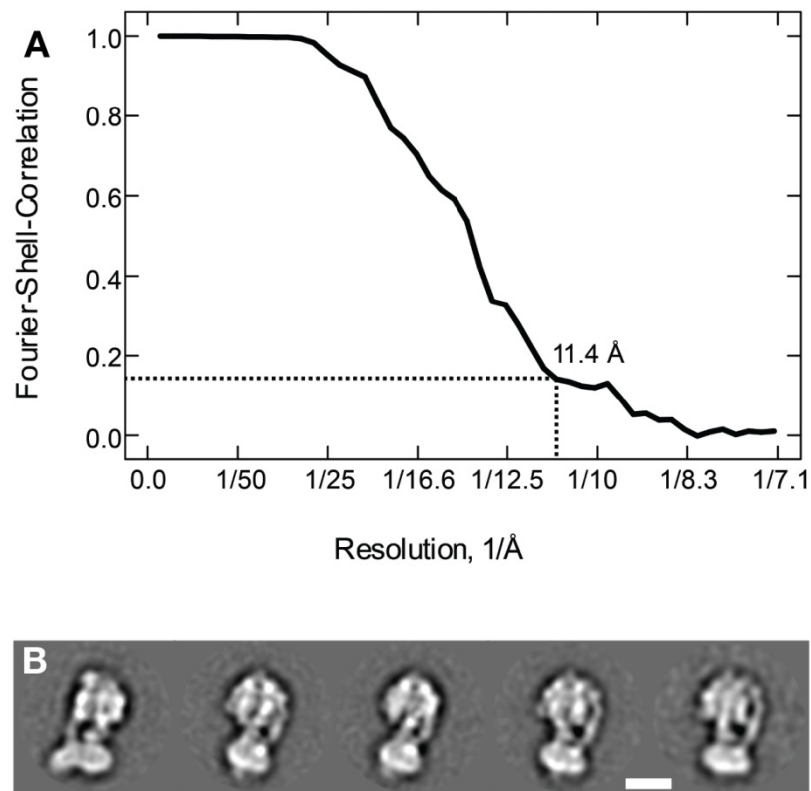
Figure S3, Related to Figure 3: Cryo-EM analysis of GraDeR-prepared bovine F_oF_1 ATP synthase.

A) "Gold-standard" Fourier shell Correlation (FSC) curve for the present cryo-EM map of bovine F_oF_1-ATP synthase indicating a resolution of about 11 Å.

B) Gallery of representative class averages of F_oF_1-ATP synthase; scalebar 10 nm.
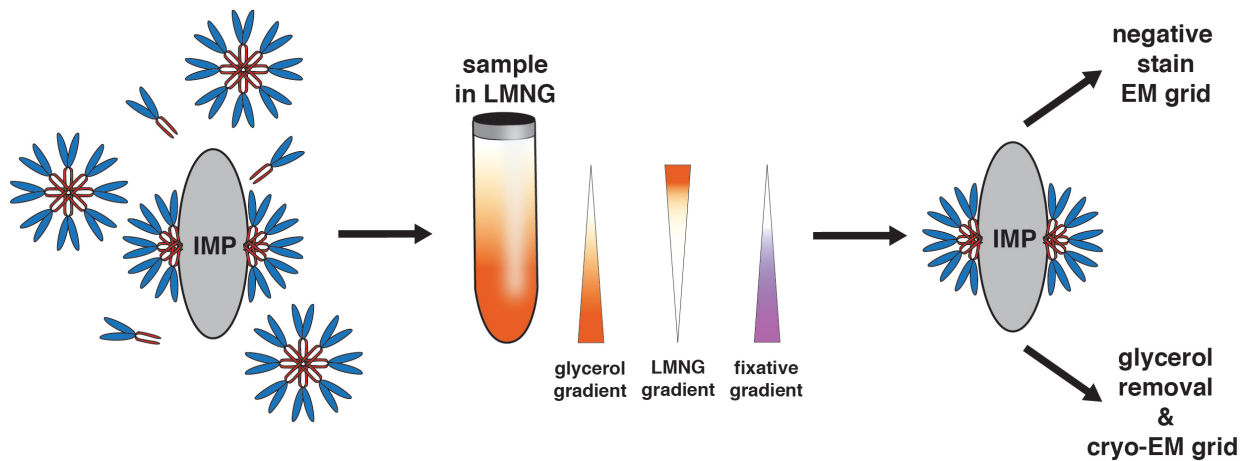
GraDeR + GraFix

Figure S4, Related to Figure 1: Combination of GraDeR with GraFix.

GraDeR can be combined with GraFix by simply adding a fixative of choice to buffer B (high concentration of crowding agent) before mixing buffer solutions A and B in the GradientMaster for gradient preparation. This would for example result in a triple gradient of 10 - 30% glycerol, 0.003 - 0% LMNG and 0 - 0.05% glutaraldehyde.

Supplemental Experimental Procedures

Model of bovine F_oF_1-ATP synthase

Molecular models of F_oF_1-ATP synthase subcomplexes from X-ray crystallography were docked into the cryo-EM density map using UCSF Chimera (Pettersen et al., 2004), i.e. models were transformed into density maps, filtered to the resolution of the EM map (11 Å) and docked as rigid bodies by optimizing correlation with the EM map. First, the most-complete subcomplex structure, the F_1-c_8 (Watt et al., 2010), entailing the αβ-hexamer, the central stalk, and c_8-ring (pdb 2XND) was docked into the EM map. The fit revealed a significant deviation between the relative orientation of αβ-hexamer and central stalk in the F_1-c_8 subcomplex and the present structure of intact F_oF_1-ATP synthase. For a substantially improved fit, the αβ-hexamer had to be docked separately from central stalk and c_8 ring resulting in a rotation of the central stalk foot region by about 30° in comparison to the crystallographic subcomplex. Such a rotation requires flexibility of the central stalk in line with results from single molecule measurements (Sielaff et al., 2008). The well-defined cryo-EM density for the αβ-hexamer indicated a further re-arrangement within the αβ-hexamer: The α and the β subunit contacting the peripheral stalk in the present complex had to be fitted separately and shifted to describe the cryo-EM map. This shift increases the distance between two β-subunits, which is corroborated by cross-linking data reported previously for the intact bacterial F_oF_1-ATP synthase in the membrane and under proton motive force (pmf) (Masaike et al., 2006). Finally, the crystal structures of the peripheral stalk (pdb 2CLY) (Dickson et al., 2006) and the oligomycin sensitivity conferral protein, "OSCP", (pdb 2WSS) (Rees et al., 2009) were docked into the EM density map. OSCP was initially placed using the full crystallographic complex including the αβ-hexamer and this fit was refined by docking the isolated OSCP.

Supplemental References

Dickson, V.K., Silvester, J.A., Fearnley, I.M., Leslie, A.G.W., and Walker, J.E. (2006). On the structure of the stator of the mitochondrial ATP synthase. Embo J *25*, 2911–2918.

Kaufmann, T.C., Engel, A. & Hervé-W. Rémigy. (2006) A novel method for detergent concentration determination. Biophys. J. *90.1*, 310-317.

Pettersen, E.F., Goddard, T.D., Huang, C.C., Couch, G.S., Greenblatt, D.M., Meng, E.C., and Ferrin, T.E. (2004). UCSF Chimera--a visualization system for exploratory research and analysis. Journal of Computational Chemistry *25*, 1605–1612.

Rees, D.M., Leslie, A.G.W., and Walker, J.E. (2009). The structure of the membrane extrinsic region of bovine ATP synthase. Proc Natl Acad Sci USA *106*, 21597–21601.

Watt, I.N., Montgomery, M.G., Runswick, M.J., Leslie, A.G.W., and Walker, J.E. (2010). Bioenergetic cost of making an adenosine triphosphate molecule in animal mitochondria. Proc Natl Acad Sci USA *107*, 16823–16827.